# REPORT DOCUMENTATION PAGE

*Form Approved*
*OMB No. 0704-0188*



| 1. REPORT DATE *(DD-MM-YYYY)* | 2. REPORT TYPE | 3. DATES COVERED *(From - To)* |
|---|---|---|
| 02-07-2008 | Technical Paper | |

**4. TITLE AND SUBTITLE**

**Energy Deposition into a Collisional Gas from Optical Lattices Formed in an Optical Cavity (Preprint)**

**5a. CONTRACT NUMBER**

**5b. GRANT NUMBER**

**5c. PROGRAM ELEMENT NUMBER**

**6. AUTHOR(S)**
T.C. Lilly (Univ. Of Colorado); S.F. Gimelshein (ERC); A.D. Ketsdever (AFRL/RZSA)
M.N. Shneider (Princeton Univ.)

**5d. PROJECT NUMBER**

**5e. TASK NUMBER**

**5f. WORK UNIT NUMBER**
**50260542**

**7. PERFORMING ORGANIZATION NAME(S) AND ADDRESS(ES)**

Air Force Research Laboratory (AFMC)
AFRL/RZSA
10 E. Saturn Blvd.
Edwards AFB CA 93524-7680

**8. PERFORMING ORGANIZATION REPORT NUMBER**

AFRL-RZ-ED-TP-2008-287

**9. SPONSORING / MONITORING AGENCY NAME(S) AND ADDRESS(ES)**

Air Force Research Laboratory (AFMC)
AFRL/RZS
5 Pollux Drive
Edwards AFB CA 93524-7048

**10. SPONSOR/MONITOR'S ACRONYM(S)**

**11. SPONSOR/MONITOR'S NUMBER(S)**
AFRL-RZ-ED-TP-2008-287

**12. DISTRIBUTION / AVAILABILITY STATEMENT**

Approved for public release; distribution unlimited (PA #08286A).

**13. SUPPLEMENTARY NOTES**
For presentation at the 26th International Symposium on Rarefied Gas Dynamics, Kyoto, Japan, 21-25 July 2008.

**14. ABSTRACT**

The Direct Simulation Monte Carlo (DSMC) method was used to investigate the interaction between argon, nitrogen, and methane test gases and ten successive pulsed optical lattices. The one-dimensional lattices were formed by two 100 ps, 393 mJ, 532 nm, laser pulses and were assumed to be far from any electronic resonance. The sequential interaction represents multiple reflections within an optical cavity or the emission of high repetition rate pulsed lasers. The maximum centerline temperature was found as a function of the intervening time between the pulses. An optimum intervening time was found and related to the mean collision time and available unexcited energy modes. The optimum time shifted proportional to the change in gas pressure, thus collision time. During sequential pulses with intervening times near zero, subsequent pulses can act to cool the gas. For pulses with intervening times longer than the optimum, thermal diffusion carries energy away from the centerline, reducing the maximum temperature. The optimal intervening time was found to be 0.7, 1.0 and 0.25 ns for argon, nitrogen, and methane at one atmosphere respectively.

**15. SUBJECT TERMS**

| 16. SECURITY CLASSIFICATION OF: | | | 17. LIMITATION OF ABSTRACT | 18. NUMBER OF PAGES | 19a. NAME OF RESPONSIBLE PERSON |
|---|---|---|---|---|---|
| a. REPORT | b. ABSTRACT | c. THIS PAGE | | | Dr. Andrew Ketsdever |
| **Unclassified** | **Unclassified** | **Unclassified** | SAR | 8 | 19b. TELEPHONE NUMBER *(include area code)* N/A |

# Energy Deposition into a Collisional Gas from Optical Lattices Formed in an Optical Cavity (Preprint)

T. C. Lilly [a], S. F. Gimelshein [b], A. D. Ketsdever [c], and M. N. Shneider [d]

[a] *University of Colorado, 1420 Austin Bluffs Parkway UH 231, Colorado Springs, CO 80933*
[b] *ERC Inc., 10 E. Saturn Blvd., Edwards AFB, CA 93524*
[c] *Air Force Research Laboratory, 10 E. Saturn Blvd., Edwards AFB, CA 93524*
[d] *Princeton University, D418 Engineering Quadrangle, Princeton, NJ, 08544*

**Abstract.** The Direct Simulation Monte Carlo (DSMC) method was used to investigate the interaction between argon, nitrogen, and methane test gases and ten successive pulsed optical lattices. The one-dimensional lattices were formed by two 100 ps, 393 mJ, 532 nm, laser pulses and were assumed to be far from any electronic resonance. The sequential interaction represents multiple reflections within an optical cavity or the emission of high repetition rate pulsed lasers. The maximum centerline temperature was found as a function of the intervening time between the pulses. An optimum intervening time was found and related to the mean collision time and available unexcited energy modes. The optimum time shifted proportional to the change in gas pressure, thus collision time. During sequential pulses with intervening times near zero, subsequent pulses can act to cool the gas. For pulses with intervening times longer than the optimum, thermal diffusion carries energy away from the centerline, reducing the maximum temperature. The optimal intervening time was found to be 0.7, 1.0 and 0.25 ns for argon, nitrogen, and methane at one atmosphere respectively.

**Keywords:**
**PACS:** 41.75.Jv, 47.70.Nd

## INTRODUCTION

The dipole, or gradient, force originates from the induced electric dipole potential of a particle in a non-uniform electric field. Since the magnitude of the force is traditionally small compared with electrostatic acceleration of ions, it has thus far found a niche in the field of low temperature atomic research. The force is routinely utilized for cooling [1], confinement [2], and transposition [3,4] of neutral atoms. In such applications, one or more laser beams are used to create a spatially varying optical potential field. If two counter-propagating beams are arranged in a manner to create an optical standing wave, the axially periodic potential formed is referred to as a one dimensional optical lattice [5]. A notional diagram of a 1D optical lattice can be seen in Figure 1. The majority of current experiments utilizing the optical dipole force use the combination of continuous wave lasers and alkali metals or meta-stable noble gases. Such combinations allow for the tuning of the laser near a well defined and isolated electronic resonance, which in turn increases the magnitude of the force in relation to a given laser intensity. Using lasers farther from resonance, the dipole force gains broader particle applicability, as it is no longer reliant on distinct electronic transitions [6], at the expense of the magnitude of the force. In order to offset the decreased magnitude, pulsed lasers can be used in lieu of continuous wave lasers to increase the optical intensity. A larger optical intensity, thus potential, translates to a larger force along the potential gradient [7,8]. Lastly, applying such high intensity, pulsed, optical lattice to a continuum gas gives the opportunity to use the dipole force as a mechanism for non-resonant energy and momentum deposition [9]. Energy deposition by way of the optical dipole force has a low ionization fraction and does not require a chemical reaction to release energy, thus changing the chemical make-up of the test species. Such gas heating can lead to non-equilibrium flow, reaction, and internal chemistry gas experiments relevant to rocket plumes [10] and space environment and spacecraft interactions.

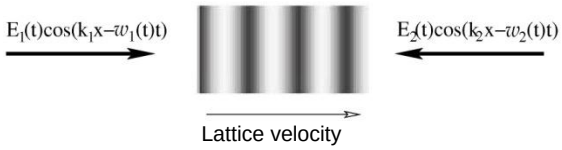


**Figure 1 Schematic of the electric field of an optical lattice**

Unfortunately the ratio of deposited energy to total laser energy is small for gases at atmospheric pressures, typically below $10^{-6}$ [9], thus most of the laser energy remains unused. An optical cavity has been suggested [11] as a means to utilize the unused energy. The task of creating a stable optical cavity with predictable and repeatable intersecting paths is non-trivial [12] and will not be addressed in the present study. However, the gas dynamic considerations for the interaction of sequential optical lattices with a single gas volume will be considered in detail. Such considerations are analogous for both lattices formed by optical cavities and those formed by a pair of high repetition rate pulsed lasers. The present study used the Direct Simulation Monte Carlo (DSMC) method to look at the thermal relaxation of translational and internal energy modes for the purpose of highlighting an optimum time between successive pulses in a multi-pulse setup. The optimum intervening time was determined by the highest temperature in the center of a gas volume after ten identical interactions between a pulsed optical lattice and the test gas. Argon, nitrogen, and methane were considered to investigate the difference between monatomic and polyatomic species.

## THEORETICAL FRAMEWORK

The interaction between an optical lattice formed by far off-resonance laser pulses and a particle within the lattice can be modelled as follows. The dipole force acting on a particle in a strong electric field is proportional to the static polarizability, α, and the gradient of the square of the electric field [13]

$$F = -\nabla U = -\frac{1}{2}\alpha\nabla\ E^{\ 2} \tag{1}$$

For anti-parallel, coherent, collimated laser pulses, the electric field in the overlapping region, as a function of space and time, can be calculated as the superposition of two counter-propagating plane waves where the square of the electric field is given by

$$E^2(x,t) = E_1^2 cos^2(k_1 x - \omega_1 t) + E_2^2 cos^2(k_2 x - \omega_2 t) + E_1 E_2\ cos((k_1 - k_2)x - (\omega_1 - \omega_2)t) + cos(k_1 + k_2)x - (\omega_1 + \omega_2)t) \tag{2}$$

where $E$, $k$ and $\omega$ are the electric field amplitude, wave number, and frequency, of the two beams. When $k_1 \approx -k_2$ and $\omega_1 \approx \omega_2$, the interference term of the field has two components: one with a relatively long spatial and short temporal period and the other with a short spatial and long temporal period. When the gradient of eqn. (2) is taken, the portion with the long spatial period has a negligible impact. In addition, the fast oscillating terms ($cos^2$) can be time averaged to a constant value. The resulting force acting on a particle within the potential region is

$$F = -\nabla U = -\frac{1}{2}\alpha\nabla\left[ E_1 E_2\ \ 1 + \cos(qx - \Omega t)\ \right] \tag{3}$$

where, $q = k_1 - k_2$ and $\Omega = \omega_1 - \omega_2$. Note that $\Omega$ and $q$ define the velocity of the optical potential standing wave, or lattice velocity, $\xi = \Omega/q$, also seen in Figure 1.

The intensity of the two laser pulses were assumed to have a Gaussian shape in both space and time which can be described by

$$I(r,t) = \mathrm{I}_{\max} e^{\left(-\frac{4\ln(2)(t - t_0)^2}{t_{\mathrm{fwhm}}^2} + -\frac{4\ln(2)r^2}{D_{\mathrm{beam}}^2}\right)} \tag{4}$$

where $t_0$ is the time at which the peak intensity will pass a spatial location and is a function of the distance from the laser, $\tau_{\mathrm{fwhm}}$ is twice the time required for the intensity to decay to half its maximum value, and $D_{\mathrm{beam}}$ is the same for radial distance. By substituting the laser intensity for the electric field magnitude eqn (3) in the axial direction becomes

$$F_x(x,r,t) = \frac{aq}{ce_0}\sqrt{I_1(x,r,t)I_2(x,r,t)}\sin(qx - \Omega t) \tag{5}$$

while in the radial direction eqn (3) becomes

$$F_r(x,r,t) = a\left(1 + \cos(qx - \omega t)\right)\frac{8\ln(2)r}{D_{\text{beam}}^2}\frac{\sqrt{I_1(x,r,t)I_2(x,r,t)}}{ce_0} \quad (6)$$

It should be noted that a gradient in the axial intensity profile caused by the temporal Gaussian shape is neglected as $(2\pi/q)/(c\,\tau_{fwhm})<<1$.

Since the laser fields are assumed to be far from a single photon resonance, the interaction between the optical lattice and the gas is limited to the translational degrees of freedom. As the dipole force is conservative, the difference in the maximum and minimum potential energy in the field, or the well depth $\Delta U$, can be related to a particle velocity which would yield a kinetic energy equal to $\Delta U$. Such a velocity is given by $v = \sqrt{2\Delta U/m}$, where $m$ is the particle mass. Reference [11] describes the effect of an optical lattice on the axial velocity distribution as limited to $\pm v$ of the lattice velocity, $\xi$. The effect within the window is a tendency towards a uniform distribution from $\xi+v$ to $\xi-v$. For laser intensities, thus lattice potentials, which correspond to a velocity range wider than the bulk of the velocity distribution, the influence of the optical lattice causes a general broadening of the distribution. From the disturbance from equilibrium accelerated particles will transfer energy to unexcited translational (and for molecular gases, internal) energy modes through collisions. The influence of the initial velocity distribution on the effect of the optical lattice interaction leads to an optimization for multi-pulse interactions in regards to the time between successive pulses and the time required for thermal relaxation.

In order to create the optimum condition for successive pulses, adequate time must be given to ensure the excited axial velocity distribution is allowed to transfer its energy to unexcited modes and relax to equilibrium. For monatomic species, the only consideration for thermal relaxation is the time required for all three translational modes to equilibrate. In order to predict the optimum time between pulses, or intervening time, the relaxation time for the disturbed distribution must be estimated. Assuming the variable hard sphere (VHS) intermolecular potential for argon at 1 atm and 300 K, the mean collision time is 137 ps [14]. Since a VHS gas needs 4 to 6 collisions to equilibrate from a large deviation from equilibrium, an optimum intervening time is expected to be about 700 ps. For the same conditions with nitrogen and methane, the time for translational relaxation is approximately 500 ps and 320 ps respectively. For molecules, internal modes must be considered. At 300 K, the number of collisions required to bring the rotational energy to within $1/e$ of the translational value, 900 ps is estimated by the VHS collision and Larsen-Borgnakke translational-internal interaction model [14]. By the same model, the vibrational relaxation is estimated at a timescale much longer than translational or rotational relaxation and much longer than thermal diffusion. Thus at temperatures lower than the characteristic vibrational temperature for nitrogen, ≈3000 K, vibrational relaxation does not influence the optimal intervening time. Thus the optimal intervening time for nitrogen should then be some time after the longest relaxation time, or >900 ps.

## SIMULATION METHOD

In order to model the interaction between a multi-pulse optical lattice and a continuum gas, simulations were conducted using a modified version of the SMILE [15] DSMC code. The SMILE code has been broadly applied, and experimentally validated, for various applications [16,17,18]. The code was extended to include the gas-optical lattice interaction. The effect of the dipole force on the particles was modelled as an instantaneous change in the particle velocity, proportional to the corresponding force at that point in time and space. Time steps were chosen sufficiently small such that the assumption of constant acceleration was valid. The force acting on the particle was determined as described above. The SMILE capabilities important for the present work are the accurate collision schemes, models for energy transfer, two-level rectangular grids different for collisions and macroparameters, radial weights for axially symmetric flows, and parallel implementation with efficient load balancing techniques. The majorant frequency scheme is employed for modeling molecular collisions [19]. The VHS model was used for modeling intermolecular interactions. The Larsen-Borgnakke model [20] with temperature-dependent rotational and vibrational relaxation numbers was utilized for rotation-translation and vibration-translation energy transfer.

The simulation domain was modelled axisymmetrically around the optical axis of two anti-parallel counter propagating laser pulses. The pulses were assumed to come from two 532 nm Nd:YAG lasers generating 393 mJ, 100 ps (full width half max) pulses focused and collimated to a diameter of 0.1 mm. In order to cover the temporal shape of the pulses, each pulse simulation ran from $\pm\,\tau_{fwhm}$, or from 100 ps before to 100 ps after the peak intensity. Simulated times with no external forces, or intervening times, were inserted between peaks as prescribed by the test. Thus peak to peak time between pulses was 200 ps plus the intervening time. The domain was assumed to be at the center of the crossing pulses and include the surrounding gas to a radius of 0.1995 mm. The distance was chosen large enough to ensure temperature and pressure perturbations did not propagate from the axis to the outer boundary

during the longest simulations. The radial boundary simulated an ambient equilibrium gas at the initial conditions. The axial domain boundaries enclosed 0.01064 mm of gas. With a laser pulse spatial length of approximately 30 mm, the axial domain boundaries were considered periodic and the domain representative of the gas at the center of the crossing region.

In order to cover a range of molecular species, argon, nitrogen, and methane were used as test gases. The polarizability to mass ratio of these gases are, 2.715, 4.24, and 10.92, [$10^{-15}$ C $m^2$ kg $V^{-1}$] respectively. The laser frequency of 532 nm can be considered far from resonance for all three species. Sampling was conducted and averaged over the last 5% of the simulation. With between 5 and 15 million simulated particles per simulation, the average numerical error for a given sampling cell is approximately 2%. Unless otherwise noted, mentioned temperatures are assumed to be at the centerline of the gas volume.

## RESULTS AND DISCUSSION

Since the pulses were modelled as Gaussian in space and the heating within the gas is proportional to the intensity of the laser field, the final translational and rotational temperature profiles of the gas for a single pulse should also be Gaussian. The result for different gases can be seen in Figure 2A. The short duration of the laser pulse does not allow for thermal diffusion to influence the profile shape over a single pulse nor allow for the internal energy modes to equilibrate with the excited translational mode. The non-equilibrium can be seen as a 200 K difference at the centerline between the methane rotational and translational modes and a 150 K difference for nitrogen. For both methane and nitrogen, the vibration modes are unexcited over a single lattice pulse. The relative magnitude of the temperature profile for each gas is consistent with the polarizability to mass ratio given in the Theoretical Framework section. As discussed earlier, the deposited energy from the lattice, thus the change in particle kinetic energy, decreases as initial gas temperature increases. Figure 2B shows the change in translational energy for one optical lattice pulse for various initial gas temperatures relative to the change at 300 K.

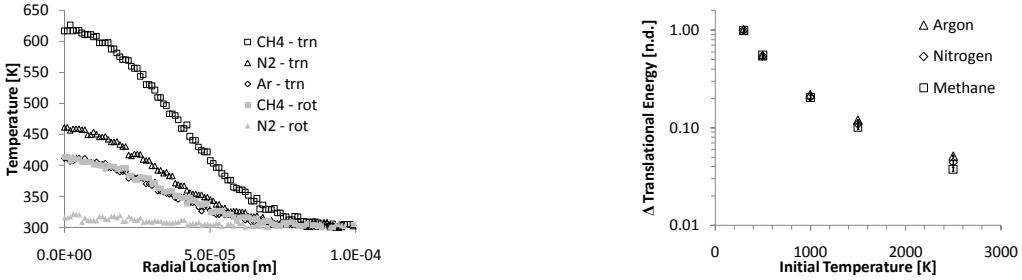


**Figure 2 (A) Translational and rotational temperature as a function of radial distance and (B) change in translational energy for varying initial temperature and a single optical lattice pulse**

Figure 3A shows the final temperature of multiple gases initially at 300 K measured at the end of 10 sequential lattice pulses with no lattice velocity. The highest temperature reached by the gas after 10 pulses is dependent on the polarizabilty to mass ratio and the available energy modes in the gas. After the first pulse, nitrogen has a higher temperature than argon, as it has a higher polarizabilty to mass. However, as the excited translational mode is allowed to relax into internal modes as well as the unexcited translational modes, argon, with less available unexcited modes, maintains a higher overall temperature. The energy deposition interacts primarily with the axial translational mode, while the relaxation of that energy will fill all available modes through collisions.

The optimum intervening time for argon is around 700 ps, consistent with the time for translational relaxation to equilibrium.

For laser intensities, thus potential wells, which affect a portion of the particle velocity distribution much less than the bulk width, ref. [9] predicts an optimum lattice velocity for the energy deposition into a continuum gas, $v_{opt} = \sqrt{2kT/m}$ . For argon at 300 K, the velocity is 353 m/s and relates to an optimization between the magnitude of the deviation from the equilibrium distribution and the total particles affected. In the present simulations, where the potential well is deep enough to affect the majority of the velocity distribution, the maximum energy deposition should occur at zero lattice velocity. The difference arises because any lattice velocity will only serve to reduce the total particles affected, without increasing the disturbance from equilibrium. To verify that the simulations adhere to the theory, the argon simulations were retested with a lattice velocity at the low-intensity theoretical maximum. As

predicted for a strong laser field, there is a slight decrease in final temperature and no change in the location of the maximum temperature versus intervening time.

As the collision frequency is linearly dependent on the number density of the gas, a proportional shift in the optimum intervening time should be observed with changing gas pressure. Figure 3B shows the shift in optimal intervening time for the centerline temperature of diatomic nitrogen originally at 300 K after 10 pulses. As expected the optimal intervening time is observed at 1 ns for 1 atm, 2 ns for 0.5 atm, and 10 ns for 0.1 atm. The maximum temperature attained after 10 pulses was not affected by the change in pressure, as the amount of energy deposited to the gas per molecule is a function of the molecular and laser properties so long as the particles are allowed to relax to thermal equilibrium after each pulse.

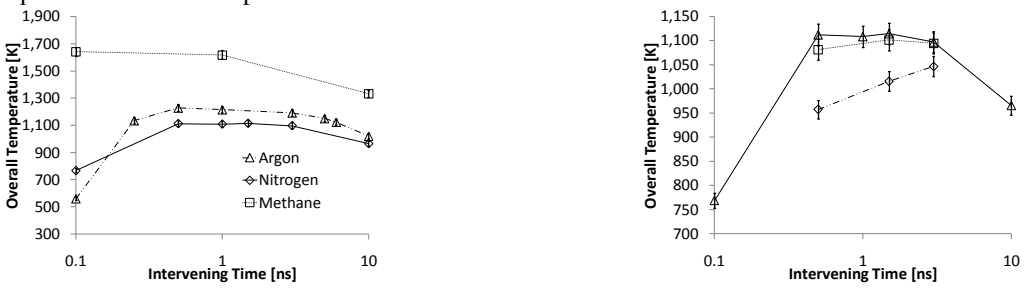


**Figure 3 Final temperature after 10 pulses as a function of intervening time for (A) several gases and (B) nitrogen at several pressures**

In addition to inadequate time for thermal relaxation, rapidly applied lattice pulses can actively decelerate gas particles for intervening times at or near zero. Figure 4A shows the temperature evolution at the centerline of the gas volume as a function of the pulse number for a zero intervening time. As expected, there is a large increase in translational temperature for the first pulse, ≈110 K. This is followed by a considerably smaller energy addition for the second pulse, ≈30 K, due to the lattice interaction with a particle velocity distribution that has already been severely disturbed. However, the third pulse shows a marked decrease in the temperature, ≈30 K. For blue-detuned lattices (lattices formed by lasers with frequencies higher than resonance), the dipole force accelerates particles towards the nodes, or peaks, in optical potential. A single 100ps pulse is not sufficiently long enough to allow a large fraction of particles to cross a distance equal to one lattice spatial period. However, by the third pulse, a large enough fraction of particles have gained a velocity towards the node and crossed to the other side. Thus the lattice during the pulse acted to decelerate the particles as the force is acting to restore them to the node. With a peak to peak time of 200 ps, the particles can expect only one collision between pulses. After the fourth pulse, the spatial distribution of particles has sufficiently aligned to the lattice potential such that there is a relatively equal number of accelerated and decelerated particles each subsequent pulse. Temperature increase is then a function of the partial thermal relaxation which the gas undergoes pulse to pulse.

Figure 4B shows the temperature evolution of the centerline of the gas volume as a function of the pulse number for a 0.5 ns intervening time with the temperature after the pulse as a diamond and the temperature after the intervening time (thus before the next pulse) as a square. There is still no significant temperature loss due to thermal diffusion during the intervening time. From the first to the tenth pulse sufficient time is given after each pulse for the gas to reach thermal equilibrium and the expected decrease in deposition efficiency is observed in a 20% less temperature increase between nine and ten then between one and two.

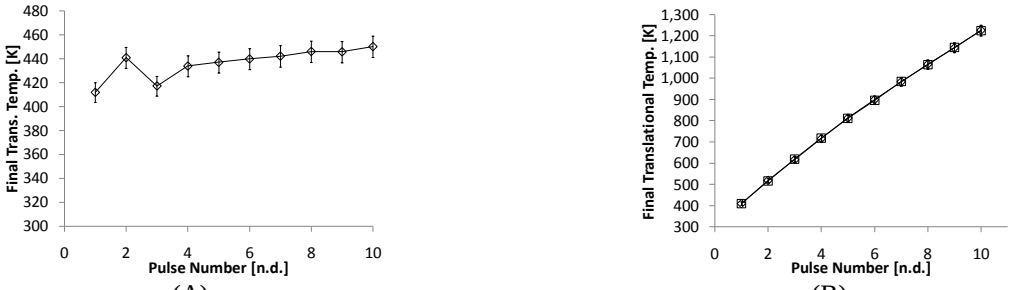


**Figure 4 Final argon translational temperature for a intervening time of (A) 0 ns and (B) 0.5 ns.**

If the intervening time is increased sufficiently, thermal diffusion mitigates the temperature increase as it allows for the flow of thermal energy away from the centerline of the gas volume. Figure 5A shows the temperature

evolution of the centerline of the gas volume as a function of the pulse number for a 10 ns intervening time. Intervening times in excess of 10-50 collisions will impart more total energy to the gas, as the lattice is interacting with a cooler gas, but at the cost of peak temperature at the centerline of the gas volume.

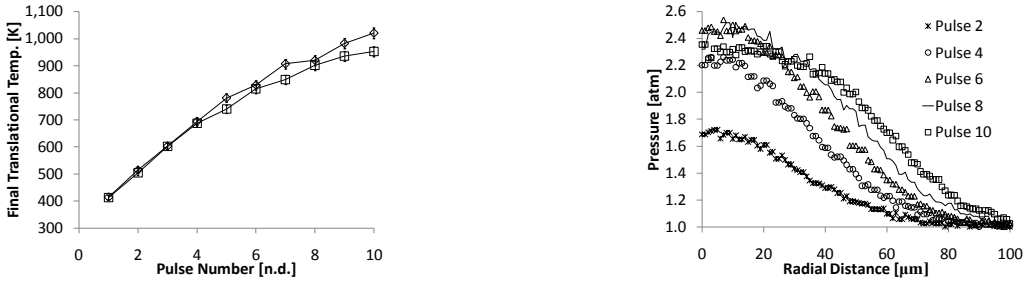


(A) (B)

**Figure 5 (A) Final argon translational temperature and (B) the pressure profile development for an intervening time of 10 ns.**

## CONCLUSION

The DSMC code SMILE was chosen and used for the present study based a history of experimentally validated results. The interaction between the three test gases and a series of 10 one-dimensional optical lattices was simulated. The optical lattices were formed by two 100 ps, 393 mJ, 532 nm, laser pulses and assumed to be far from any electronic resonance. The intervening time between the pulses was varied to investigate the optimization of the energy deposition from the optical lattice to the gas. An optimal intervening time was found and related to the mean collision time for a monatomic, diatomic, and polyatomic species. For intervening times near zero, the interaction between subsequent optical lattices and the disturbed gas can cause active gas cooling. For intervening times much greater than the optimum, thermal diffusion acts to transport energy away from the centerline, reducing the highest temperature reached by the gas. Using the centerline temperature after 10 pulses, the optimal intervening time was found to be 0.7, 1.0 and 0.25 ns for argon, nitrogen, and methane respectively.

## ACKNOWLEDGEMENTS

This work has been supported by the Air Force Research Laboratory at Edwards AFB, CA and the Air Force Office of Scientific Research. The authors wish to thank Dr. Ingrid Wysong for her continued support and input.

## REFERENCES

1 Chen et al., "Adiabatic Cooling of Atoms by an Intense Standing Wave," *Physical Review Letters* **69**, (1992), pp. 1344-1347
2 Kuga et al., "Novel Optical Trap of Atoms with a Doughnut Beam," *Physical Review Letters* **78**, (1997), pp. 4713-4716
3 Dotsenko et al., "Submicrometer Position Control of Single Trapped Neutral Atoms," *Physical Review Letters* **95**, (2005), pp. 033002-1 - 033002-4
4 Schrader et al., "An optical conveyor belt for single neutral atoms," *Applied Physics B* **73**, (2001), pp. 819-824
5 Metcalf, Harold J. & van der Straten, Peter, *Laser Cooling and Trapping*, New York, Springer, 1999
6 Takekoshi T., et al., "Quasi-electrostatic trap for neutral atoms," *Optical Communications* **114**, (1995), pp. 421-424
7 Pan, Xingguo, et al., "Coherent Rayleigh-Brillouin scattering in molecular gases," *Physical Review A* **69**, (2004), Article 033814
8 Sakai, Hirofumi, et al., "Optical deflection of molecule," *Physical Review A* **57**, (1998), pp. 2794-2801
9 Ngalande C., Gimelshein S. F. and Shneider M. N., "Energy and momentum deposition from pulsed optical lattices to nonionized gases," *Applied Physics Letters* **90**, (2007), pp. 121130-1 - 121130-3
10 Simmons F. S., *Rocket Exhaust Plume Phenomenology*, (2000) Aerospace Press Series, AIAA
11 Shneider M. N. and Barker P. F., "Optical Landau damping," *Physical Review A* **71**, (2005), pp. 053403-1 - 053403-9
12 Rollason A. J., et al., "Multipass optical cavity for inverse Compton interactions," *Nuclear Instruments & Meathods in Physics Research A* **526**, (2004), pp. 560-571
13 Boyd, Robert W., *Nonlinear Optics*, San Diego, Academic Press, Inc., 1992, 1st Edition, p. 328
14 Bird, G. A., *Molecular Gas Dynamics and the Direct Simulation of Gas Flows*, Oxford, Clarendon Press, 1995

[15] Ivanov M.S., Kashkovsky A.V., Gimelshein S.F., Markelov G.N. "Statistical simulation of hypersonic flows from free-molecular to near-continuum regimes" *Thermophysics and Aeromechanics* **4**, (1997), pp. 251-268.

16 Lilly T. C., Gimelshein S. F., Ketsdever A. D., and Markelov G. N., "Measurements and computations of mass flow and momentum flux through short tubes in rarefied gases," *Phys. Fluids* **18,** (2006), Article 093601

17 Lilly T. C., Duncan J. A., Nothnagel S. L., Gimelshein S. F., Gimelshein N. E., Ketsdever A. D., and Wysong I. J.,, "Numerical and experimental investigation of microchannel flows with rough surfaces," *Phys. Fluids* **19,** (2007), Article 106101

18 Ivanov M.S., et al., "High-Altitude Capsule Aerodynamics with Real Gas Effects," *J. of Spacecraft and Rockets* **35**, (1998) pp. 16-22.

19 Ivanov, M.S., and Rogasinsky, S.V., "Analysis of the numerical techniques of the direct simulation Monte Carlo method in the rarefied gas dynamics," *Soviet J. Numerical Analytical Math. Modeling* **3**, (1988) pp.453-465.

20 Borgnakke, C., and Larsen, P.S., "Statistical collision model for Monte Carlo simulation of polyatomic gas mixture," *J. Comp. Phys.* **18**, (1975), pp.405-420.